This study investigates the process of analyzing immunohistochemical images of breast cancer. The study has contributed to solving the task of a standardized and objective approach to the quantitative assessment of immunohistochemical biomarkers, which would minimize inter-individual variability in assessments and could be computationally efficient for the analysis of biomedical images.

This paper aims to balance model complexity and generalization by using evolutionary algorithms to tune deep neural networks for biomedical tasks, analyzing how network structure affects performance.

Experiments were conducted on the segmentation of immunohistochemical images on 13 different architectures of neural networks. The evaluation was performed using five accuracy metrics, which allowed for an objective comparison of model performance. The use of a genetic algorithm to optimize the neural network architecture made it possible to adaptively find combinations of parameters, in particular the number of layers and the size of the base filter. The evolutionary approach enabled effective exploration of configuration space, which led to an increase in the Dice metric to 0.74. The resulting increase in accuracy indicates the model's improved ability to segment images with different characteristics, demonstrating the practical effectiveness of the proposed approach for biomedical diagnosis tasks.

The optimized architecture was used to design a system for diagnosing breast cancer automatically based on neural networks, in particular for the method of automatic diagnosis of breast cancer subtypes. That contributed to improving the accuracy of biomedical image analysis, which could help improve the diagnostic process in clinical practice

Keywords: Attention U-Net, genetic algorithm, neural network architecture optimization, IHC images, biomedical image segmentation, automatic diagnosing of breast cancer

UDC 004.8
DOI: 10.15587/1729-4061.2025.344041

DEVISING A COMPREHENSIVE APPROACH TO DIAGNOSING BREAST CANCER SUBTYPES AUTOMATICALLY BASED ON DEEP NEURAL NETWORKS

Oleh Berezsky
Corresponding author
Doctor of Technical Sciences*
E-mail: olber62@gmail.com
Pavlo Liashchynskyi
Lecturer, PhD Student*
Petro Liashchynskyi
Doctor of Philosophy (PhD)
Department of Automated Control Systems
Lviv Polythechnic National University
S. Bandery str., 12, Lviv, Ukraine, 79013
Petro Selskyy
Doctor of Medical Sciences
Department of Pathologic Anatomy,
Autopsy Course and Forensic Pathology
I. Horbachevsky Ternopil National Medical University
of the Ministry of Health of Ukraine
Maydan Voli, 1, Ternopil, Ukraine, 46001
*Department of Computer Engineering
West Ukrainian National University
L'vivs'ka str., 11, Ternopil, Ukraine, 46009

Received 01.09.2025
Received in revised form 03.11.2025
Accepted 12.11.2025
Published 30.12.2025

How to Cite: *Berezsky, O., Liashchynskyi, P., Liashchynskyi, P., Selskyy, P. (2025). Devising a comprehensive approach to diagnosing breast cancer subtypes automatically based on deep neural networks. Eastern-European Journal of Enterprise Technologies, 6 (2 (138)), 15–25. https://doi.org/10.15587/1729-4061.2025.344041*

1. Introduction

In the modern world, artificial intelligence (AI) is rapidly penetrating various areas of human activity, in particular medicine [1, 2]. One of the most promising and relevant field of its application is to automatically diagnose diseases using biomedical images [3]. AI makes it possible to increase the accuracy, quality, and efficiency of the diagnostic process, reducing the influence of the human factor.

Of particular note is the use of deep neural networks for the analysis of histopathological [4, 5] and immunohistochemical (IHC) [6, 7] images for diagnosing breast cancer [8]. Histopathological images make it possible to identify the presence of cancer cells, while IHC studies make it possible to detect protein markers that play an important role in determining the cell type and molecular genetic subtype of the tumor. For this purpose, antibodies are used that bind to the corresponding proteins, and the results are visualized using special dyes.

It is important that determining the subtype of breast cancer has not only diagnostic but also therapeutic significance. It is based on the analysis of four main biomarkers (ER, PgR, Ki67, HER2), which correspond to the following subtypes: luminal A, luminal B, HER2-positive, and basal-like (triple-negative). In the diagnostic process, four corresponding IHC images are usually used for one histopathological image,

Copyright © 2025, Authors. This is an open access article under the Creative Commons CC BY license

which are evaluated by two main parameters: average staining intensity and percentage of positive cells.

According to statistics [9, 10], breast cancer is a fairly common oncological disease. The development of accurate deep learning models for automatic analysis of biomedical images of breast cancer makes it possible not only to speed up the diagnosis but also reduce the likelihood of errors associated with the subjective assessment by the doctor.

At the current stage of development of medical information systems, one of the urgent tasks is the accurate segmentation of micro-objects on histological and IHC images. A significant part of the research in this area is focused on using the U-Net architecture as a basis for building automatic segmentation systems. The popularity of the architecture is explained by the ability to effectively detect objects of different sizes even on small training samples [11].

Despite significant progress, existing diagnostic methods face certain difficulties. First, subjective assessment of IHC images by clinicians often leads to significant variability in the results, especially for the Ki67 proliferation index. Studies confirm that the interlaboratory reproducibility of Ki67 is only moderate, with an intraclass correlation coefficient ranging from 0.59 to 0.71. The geometric mean value of Ki67 for each laboratory in 100 cases ranged from 7.1% to 23.9% for central staining and from 6.1% to 30.1% for local staining [12]. Second, the analysis of large image samples is resource-intensive and time-consuming. Infrastructural limitations and the high cost of WSI (Whole Slide Imaging) scanners create barriers to their widespread implementation and AI algorithms in clinical practice [13]. These limitations necessitate the development of automated solutions that can provide both high segmentation accuracy (on small, computationally efficient fragments) and automatically convert these segmentation results into standardized quantitative biomarker estimates necessary for accurate molecular subtyping.

In this context, the use of genetic algorithms for automatic optimization of neural network architecture opens up opportunities to improve the accuracy and stability of results. The use of a genetic approach makes it possible to select network parameters for specific biomedical data. The results obtained make it possible to reduce the time for analyzing IHC images, reduce the subjectivity of evaluation, and provide more accurate tumor definition.

Therefore, research to devise an integrated method for diagnosing breast cancer automatically based on optimized neural networks has high practical value and is relevant. The results could be directly integrated into automatic diagnostic systems, providing standardized and rapid quantitative assessment.

2. Literature review and problem statement

In [14], the results from analyzing the following U-Net architectures are reported: Basic U-Net, 3D U-Net, Attention U-Net, Inception U-Net, Residual U-Net, Recurrent U-Net, Dense U-Net, U-Net++, Adversarial U-Net, and Ensemble U-Net. The work compares the above architectures and their alternatives. However, the authors did not investigate the influence of network depth and filter size and did not assess the stability of the models on IHC images, which limits the generalization of the results.

In [15], the effectiveness of 3D U-Net for brain tumor segmentation was demonstrated, in which the average Dice coefficient was 0.87, and in the modified version [16] – 0.89. Despite the high accuracy for three-dimensional MRI images, the authors did not check the generalizability of the architecture on 2D IHC data, which have significantly different texture and colorimetry. This creates a need to adapt U-Net to flat biomedical images.

This approach is used in [17] but it focuses on specific segmentation tasks rather than comprehensive analysis. In it, the segmentation of protein expression in the membrane region – HER2 of breast cancer was demonstrated using different segmentation models: FCN, SegNet, and U-Net. The best results were shown by U-Net (94% accuracy, F1 = 0.91) but the model had low stability when overlapping cells, which reduced Dice to 0.78. Improving this architecture by means of residual or attention blocks could improve the quality of nuclear separation in dense areas.

This approach is used in [18], in which the authors propose a new model Attention-Enhanced and Residual U-Net for segmentation of protein-expressed nuclei in an aberrant cell. The proposed approach increased the segmentation accuracy by 4–6% compared to the basic U-Net, reaching Dice up to 0.83 on IHC images. At the same time, the problem of segmentation of overlapping cells remained unsolved. An option to overcome such difficulties may be morphological post-processing of segmented micro objects. This is the approach used in [19]. The method accurately selects the nuclei of the shaded area of breast tissue images, but its effectiveness has not been confirmed on a wide range of data.

In [20], segmentation methods based on different types of neural networks are described: U-Net, R-CNN, and the developed GB U-Net. GB U-Net showed an accuracy of 0.88, but when changing the tissue type, it dropped to 0.79, which indicates limited generalization ability. To overcome this, in [21] a universal model GeNSeg-Net was proposed, which on different IHC sets kept Dice within 0.84–0.87 even on small samples.

In [22], a pixel-level approach for classifying HER2 receptor expression was described (accuracy 91%), however, the model does not integrate data from other markers (ER, PgR, Ki67), which limits its clinical ability. This emphasizes the need for a comprehensive method that would combine the analysis of histopathological and IHC images for full-fledged molecular subtyping.

Thus, our review of related literature demonstrates that existing U-Net architectures provide high quality local segmentation but do not take into account interlaboratory differences and are not integrated into a complete diagnostic pipeline. This suggests that it is appropriate to conduct a study aimed at devising an automatic method for diagnosing breast cancer that combines the analysis of histopathological and IHC images.

3. The aim and objectives of the study

The aim of our research is to devise a comprehensive approach to diagnosing breast cancer subtypes automatically, combining segmentation of IHC images and classification of histopathological data. This will improve the diagnosing quality, reduce the influence of the human factor in making a diagnosis, and enable high-quality image processing under conditions of limited computing resources.

To achieve the goal, the following tasks were set:

– to optimize the architecture of U-Net networks for segmenting IHC images;

– to devise a method for automatic determination of informative parameters of IHC images and identification of breast cancer subtypes.

4. The study materials and methods

The object of our study is the process of analyzing IHC images of breast cancer.

The principal hypothesis assumes that automatic segmentation of IHC images, determination of informative parameters and identification of subtypes of breast cancer could improve the accuracy of diagnosing and reduce the influence of the human factor. This hypothesis was based on a number of assumptions, namely:

– comparison of different modifications of the U-Net architecture on the same set of test data with a fixed number of training epochs will make it possible to determine the model with the best segmentation quality;

– further optimization using a genetic algorithm will contribute to increasing the accuracy of segmentation of IHC images of breast cancer.

At the same time, a number of simplifications were adopted in the research process, namely:

– a fixed number of training epochs was used to compare U-Net models;

– the pre-processing process (color normalization, noise removal, scaling) was considered sufficient and did not change between experiments;

– the use of a genetic algorithm to optimize model parameters was limited to a fixed number of generations and population size;

– external clinical factors were not taken into account (age, sex, stage of disease), since the study focuses only on image analysis;

– all images were assumed to have similar staining conditions (same IHC method and biomarker intensity).

The method for diagnosing automatically consists of the following stages (Fig. 1):

– automatic classification of histopathological images;

– automatic segmentation of IHC images;

– automatic identification of breast cancer subtypes.

Our study was conducted on a private dataset provided by the Department of Pathological Anatomy at Ternopil National Medical University. The dataset includes histological images divided into three classes (G1, G2, G3) and four series of IHC images (ER, PgR, HER2, Ki67) of breast cancer used for molecular subtyping.

The original IHC images had a resolution of 4096×3286 pixels. The training sample included 19 samples, the test sample – 13. To increase the number of examples, the images were cut into fragments of 128×128 pixels. That is, the images were not proportionally scaled to the given size, as this would lead to the loss of structural details. As a result, 759 training samples, 223 test samples, and 20% of the training sample were allocated for validation.

Image quality depends on the staining standard and the characteristics of the microscope or sensor (e.g., uneven illumination and chromatic aberrations). The possible influence of dyes was also considered as a factor in the color variability between series. The influence of interlaboratory differences was partially minimized by colorimetric augmentations (change in brightness, contrast, color shift) and intensity normalization before starting. No geometric augmentations were applied to the images.

An example of a histopathological image and its four corresponding IHC images is shown in Fig. 2. The original images are borrowed from [23].

For automatic classification of histopathological images of breast cancer, developed CNN architecture was used. For tissue classification, classes G1, G2, and G3 are used, which correspond to different levels of differentiation and aggressiveness.

13 neural network architectures were selected for automatic segmentation. This choice is due to the need to conduct a comprehensive evaluation of different architectural approaches in order to assess their impact on the accuracy of segmentation of IHC images. These architectures are given in Table 1.

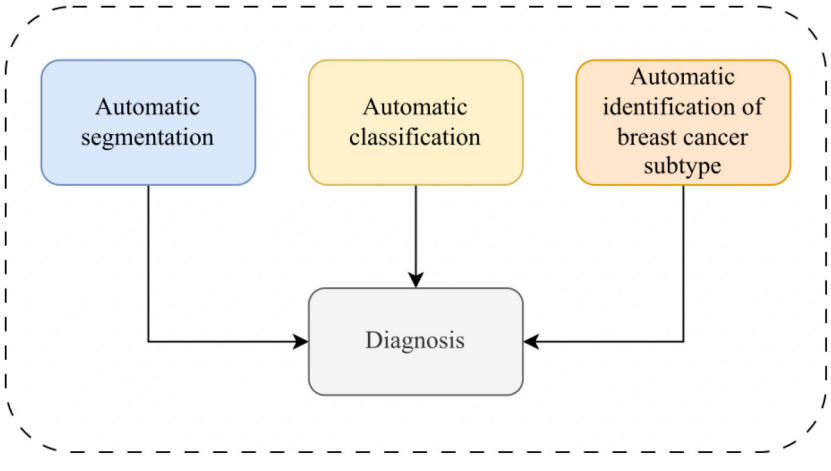

Fig. 1. General scheme of the method for diagnosing automatically

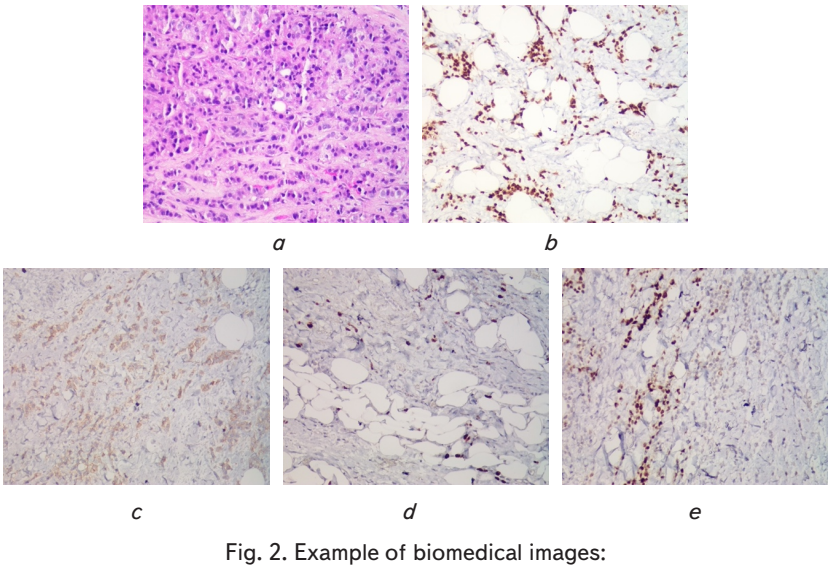

Fig. 2. Example of biomedical images:
a – histopathological; *b* – immunohistochemical ER (estrogen receptor); *c* – immunohistochemical HER2 (human epidermal growth factor receptor 2); *d* – immunohistochemical Ki67 (proliferation index); *e* – immunohistochemical PgR (progesterone receptor)

Table 1

Selected architectures

No.	ID
1	Base U-Net
2	ResNet
3	WideResNet
4	ResNeXt
5	RegNet
6	AlexNet
7	VGG-16
8	DenseNet
9	Attention U-Net
10	GoogLeNet
11	Inception V3
12	EfficientNet
13	EfficientNetV2

The classical U-Net architecture was taken as a basis, which consists of two main modules: encoder and decoder [11]. This architecture is given in Fig. 3. All other architectures were used as backbone.

The segmentation process is illustrated by the general structure shown in Fig. 4. Pairs of original images and corresponding segmentation masks are used to train the network. After training, the model is saved and used to segment new test data. The result is segmented images that can be used for further analysis.

The following metrics were used to assess the segmentation accuracy: Dice coefficient (DC), Precision & Recall, Jaccard index (also known as IoU), and Accuracy [25]. To detail the metrics, we introduce the following notations:

– *TP* – true positive,

– *TN* – true negative,

– *FN* – false negative,

– *FP* – false positive.

Precision score is the number of true positives divided by the number of all positives. The metric is described by formula (1)

$$\text{Precision} = \frac{TP}{TP + FP}. \quad (1)$$

The Recall score metric is the number of true positives divided by the number of all samples that should have been identified as positive. The metric is described by formula (2)

$$\text{Recall} = \frac{TP}{TP + FN}. \quad (2)$$

The Accuracy score metric is the number of correct predictions, consisting of correct positive and negative predictions, divided by the total number of predictions. The metric is described by formula (3)

$$\text{Accuracy} = \frac{TP + TN}{TP + TN + FN + FP}. \quad (3)$$

The F-measure is one of the most common performance metrics in computer vision.

The DC coefficient is calculated based on the accuracy and reproducibility of the prediction. This coefficient then evaluates the agreement between the predicted and true segmentation. The coefficient also takes into account false positives, which is a common factor in multi-class unbalanced datasets.

Based on the F-measure, there are two popular metrics used for biomedical image segmentation:

1) Jaccard index or IoU;

2) DC is the most widely used metric in the vast majority of scientific publications for segmentation evaluation.

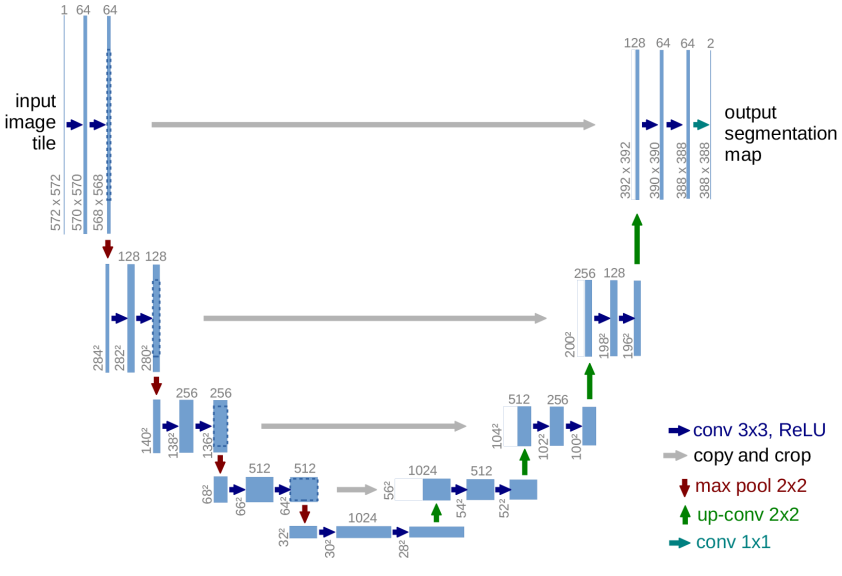

Fig. 3. U-Net architecture (example for a 32 × 32 pixel image) [11]

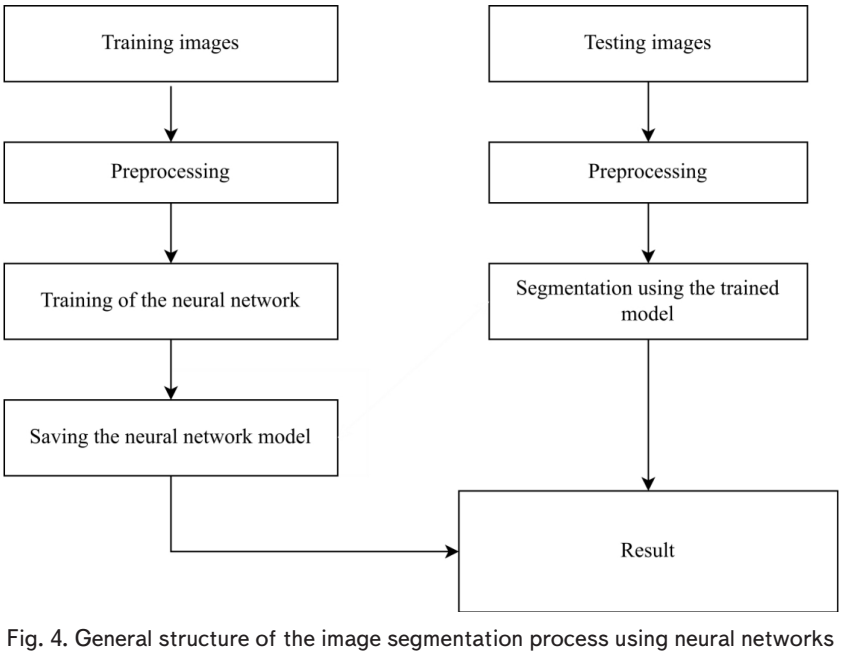

Fig. 4. General structure of the image segmentation process using neural networks

So, DC is the harmonic mean of accuracy and reproducibility. This metric is described by formula (4)

$$\mathrm{DC} = \frac{2TP}{2TP + FP + FN}. \quad (4)$$

Jaccard index or IoU is the area of intersection over the union of the predicted segmentation and the ground truth. The metric is described by formula (5)

$$\mathrm{IoU} = \frac{TP}{TP + FP + FN}. \quad (5)$$

DC was chosen as the main metric because it effectively measures spatial overlap, handles class imbalance well, and provides a balanced assessment of segmentation accuracy and completeness.

The architecture was optimized using NNI (Neural Network Intelligence) tools. 50 trials were conducted, each lasting 150 epochs. The network parameters were varied, such as the number of layers (affecting its depth), the size of the base filter (affecting feature analysis), and the learning rate, which in certain trials, selected randomly, gradually decreased by a factor of 10 after every 50 epochs. This allowed the learning to stabilize at the final epochs.

The range for the number of layers was from 3 to 8, and for the filter size – from 16 to 256 pixels. The images were reduced to a size of 128×128 pixels. For example, if we take a basic filter with a size of 64 pixels and the number of layers is 6, then the last sixth layer of the encoder will have a dimension of 2048×4096 pixels.

The clinicopathological surrogate classification of the breast cancer subtype is determined based on the results of IHC studies for four main biomarkers: ER, PgR, HER2, Ki67.

The diagnosis is made based on the rules and characteristics that are given in [26, 27].

The formalized base of production rules is given in Table 2.

It is worth noting that to increase the significance of the results in an international context, the formalized base of production rules is also based on international recommendations, in particular the Consensus of the European Society of Medical Oncology (ESMO) [28].

The interaction of the expert system components for this task occurs according to a cyclic process of "pattern matching". At the beginning, the initial clinical data of the patient (ER, PgR, HER2, and Ki67 status) are loaded into the working memory. Next, the interpreter of the system begins its cycle:

1. Image selection: the interpreter focuses on the data in the working memory.

2. Matching: it reviews the entire rule base (RULE-01... RULE-05) and matches the prerequisites of each rule with the data in the working memory. This leads to the formation of the so-called "conflict set" – a list of all rules whose prerequisites are satisfied by the current data.

3. Conflict resolution: given the hierarchical nature of the classification described in Section 3, this step is critically important. Let's imagine that for a tumor that is ER positive and HER2 positive, two rules can be triggered simultaneously: one that looks for only HER2 positive and another that looks for ER positive AND HER2 positive. To avoid misclassification, the inference mechanism must have a clear strategy. The most logical strategy is the "longest match" strategy, which prioritizes the rules with the most satisfied conditions. This ensures that the system will choose the most specific and accurate rule that follows the logic of the diagram.

4. Rule execution: After resolving the conflict, the system executes the selected rule, which results in the addition of a new fact – the specified cancer subtype – to the working memory. If only one matching subtype is found, the process is terminated.

This mechanism ensures consistent and logically correct inference, allowing the system to go from the initial clinical data to the final diagnostic conclusion.

The structure of an expert system based on a production model is shown in Fig. 5.

Ki67 values should be interpreted in the context of local laboratory values: for example, if a laboratory has a mean Ki67 score of 20% for receptor-positive disease, values of 30% or higher may be considered clearly high; values of 10% or lower may be considered clearly low.

"Triple-negative" also includes some special histological types, such as lymphoma-rich stromal carcinoma (previously called medullary), secretory carcinoma, low-grade metaplastic carcinoma, and adenoid cystic carcinoma [26].

The Python programming language and PyTorch framework were used for the experimental part of the study. Computational experiments were performed in the Jarvislabs and Kaggle cloud environments using NVIDIA Quadro RTX5000 and two T4 GPUs, respectively.

The NNI library was used for automated search for the optimal architecture.

To determine the computational features, the OpenCV, numpy, and scikit-image libraries were used.

Table 2

Formalized base of production rules

ID	IF	THEN
RULE-01	ER is positive (≥ 1%) AND HER2 is negative (≤ 10% staining) AND PgR is high (≥ 20%) AND Ki67 is low (< 10%)	Subtype is Luminal A-like
RULE-02	ER is positive (≥ 1%) AND HER2 is negative (≤ 10% staining) AND (PgR is low (< 20%) OR Ki67 is high (≥ 30%))	Subtype is Luminal B-like (HER2-negative)
RULE-03	ER is positive (≥ 1%) AND HER2 is positive (> 10% staining)	Subtype is Luminal B-like (HER2-positive)
RULE-04	HER2 is positive (> 10% staining) AND ER is negative (< 1%) AND PgR is negative (< 1%)	Subtype is HER2-positive (non-luminal)
RULE-05	ER is negative (< 1%) AND PgR is negative (< 1%) AND HER2 is negative (≤ 10% staining)	Subtype is Basal-like (triple-negative)

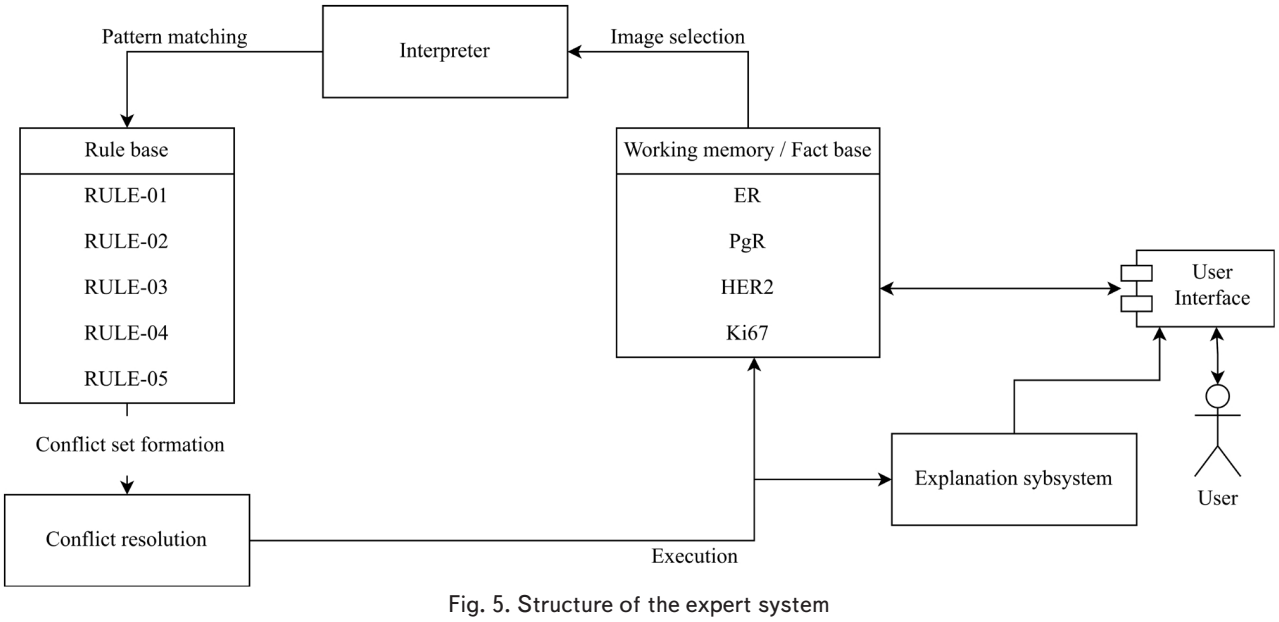

Fig. 5. Structure of the expert system

5. Results of devising a comprehensive method for diagnosing breast cancer subtypes automatically

5. 1. Optimization of the U-Net architecture

The architecture optimization procedure is shown in Fig. 6.

The following are five sequential steps that implement the evolutionary search for the optimal configuration of hyperparameters:

1. Initialization. At this step, the basic parameters of the model are set, such as the size of the initial filter, the number of layers, and the learning rate.

2. Hyperparameter search. This stage includes automatic testing of different hyperparameter variants to find the best configuration.

3. Training. The model is trained with the specified parameters. At each step, the weights are adjusted using backpropagation of the error.

4. Evaluation. At this stage, metrics are calculated after each epoch, which allows determining the effectiveness of the model on the validation data.

5. Optimization. This stage is the final one. Here, NNI selects the best parameters based on DC. After that, it starts from step 2. This makes it possible to improve the performance of the model in the following stages. This continues until the desired accuracy is found or the resources for finding the optimal architecture are exhausted.

Table 3 gives results from comparing the accuracy metrics for the 13 selected architectures. The data is sorted in descending order by the DC metric.

As can be seen from Table 3, the best DC results are obtained by the Attention U-Net architecture, which is why it was selected for optimization by the genetic algorithm.

Table 4 displays the DC metric results for the 13 selected architectures and the optimized version of Attention U-Net.

Table 5 gives the statistical impact of Attention U-Net's optimized hyperparameters.

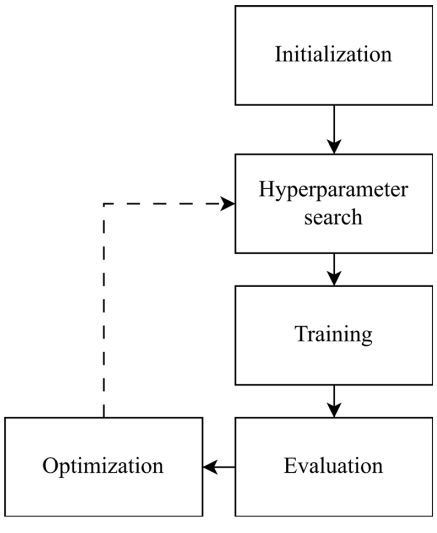

Fig. 6. Architecture optimization procedure

Table 3

Results of comparing segmentation accuracy metrics

No.	ID	DC	IoU	Accuracy	Precision	Recall
1	Attention U-Net	0.728995	0.60248	0.941858	0.955794	0.790606
2	Base U-Net	0.726499	0.5965	0.941439	0.9998	0.9997
3	VGG-16	0.708442	0.575997	0.940182	0.958385	0.895585
4	DenseNet	0.707411	0.566541	0.938797	0.934624	0.849893
5	ResNet	0.681889	0.552199	0.932116	0.972939	0.853237
6	WideResNet	0.678025	0.543014	0.933921	0.981421	0.886418
7	RegNet	0.586989	0.419881	0.911491	0.783565	0.564647
8	ResNeXt	0.571013	0.408371	0.91245	0.794248	0.536481
9	GoogLeNet	0.526026	0.361661	0.90075	0.833287	0.540659
10	EfficientNetV2	0.511565	0.34633	0.899231	0.677133	0.466727
11	EfficientNet	0.39894	0.241527	0.88585	0.595445	0.332688
12	AlexNet	0.234396	0.138411	0.878506	0.519243	0.233029
13	InceptionV3	0.166613	0.096877	0.878474	0.386335	0.163947

Table 4

Best DC results for U-Net architectures

Name	Base filter size	Num layers	Max DC	Learning rate
Optimized Attention U-Net	32	6	0.7400	1e-3
Base Attention U-Net	64	4	0.7289	1e-3
Base U-Net	64	4	0.7264	1e-3
VGG-16	64	16	0.708442	1e-3
DenseNet	64	121	0.707411	1e-3
ResNet	64	50	0.681889	1e-3
WideResNet	64	50	0.678025	1e-3
RegNet	32	79	0.586989	1e-3
ResNeXt	64	5	0.571013	1e-3
GoogLeNet	64	22	0.526026	1e-3
EfficientNetV2	32	50	0.511565	1e-3
EfficientNet	32	18	0.39894	1e-3
AlexNet	11	8	0.234396	1e-3
InceptionV3	32	48	0.166613	1e-3

Table 5

Statistical impact of optimized Attention U-Net hyperparameters

ID	Base filter size	Num layers	Max DC	Average DC	Deviation DC	DC growth relative to Base, %
Base Attention U-Net	64	4	0.7289	0.7180	0.0051	–
Optimized Attention U-Net	32	6	0.7400	0.7350	0.0033	+1.5
Optimized Attention U-Net v2	8	16	0.7295	0.71	0.0089	+0.1
Optimized Attention U-Net v3	3	128	0.6901	0.675	0.0045	-5.3

Fig. 7 shows the segmentation results using Attention U-Net. The original image is taken from [23].

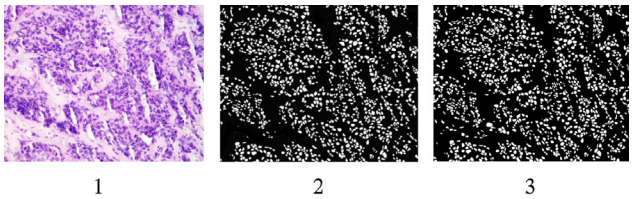

1 2 3

Fig. 7. Results of Attention U-Net models:
1 — original IHC image; 2 — segmented by Base Attention U-Net architecture; 3 — segmented by Optimized Attention U-Net architecture

The structure of the Attention U-Net architecture encoder is shown in Fig. 8. Each block corresponds to a 3 × 3 convolution with a certain number of channels.

The class diagram of the implemented segmentation software module is shown in Fig. 9. The module implements the optimized architecture of Optimized Attention U-Net.

The implemented classes provide a structured representation of the components of a neural network model for IHC image segmentation. Their use contributes to the unification of approaches to data processing, training, and model evaluation, which facilitates analysis, optimization, and interpretation of results. This, in turn, increases the accuracy and reliability of research results.

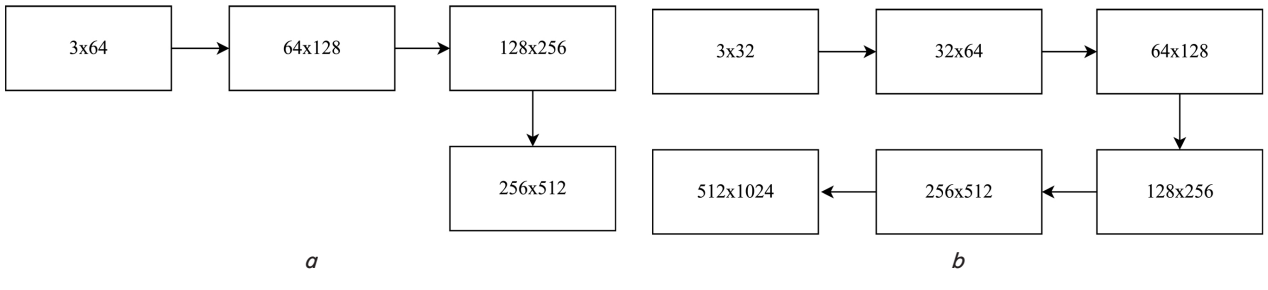

Fig. 8. Encoder structure:
a — basic Attention U-Net architecture; *b* — its optimized version Optimized Attention U-Net

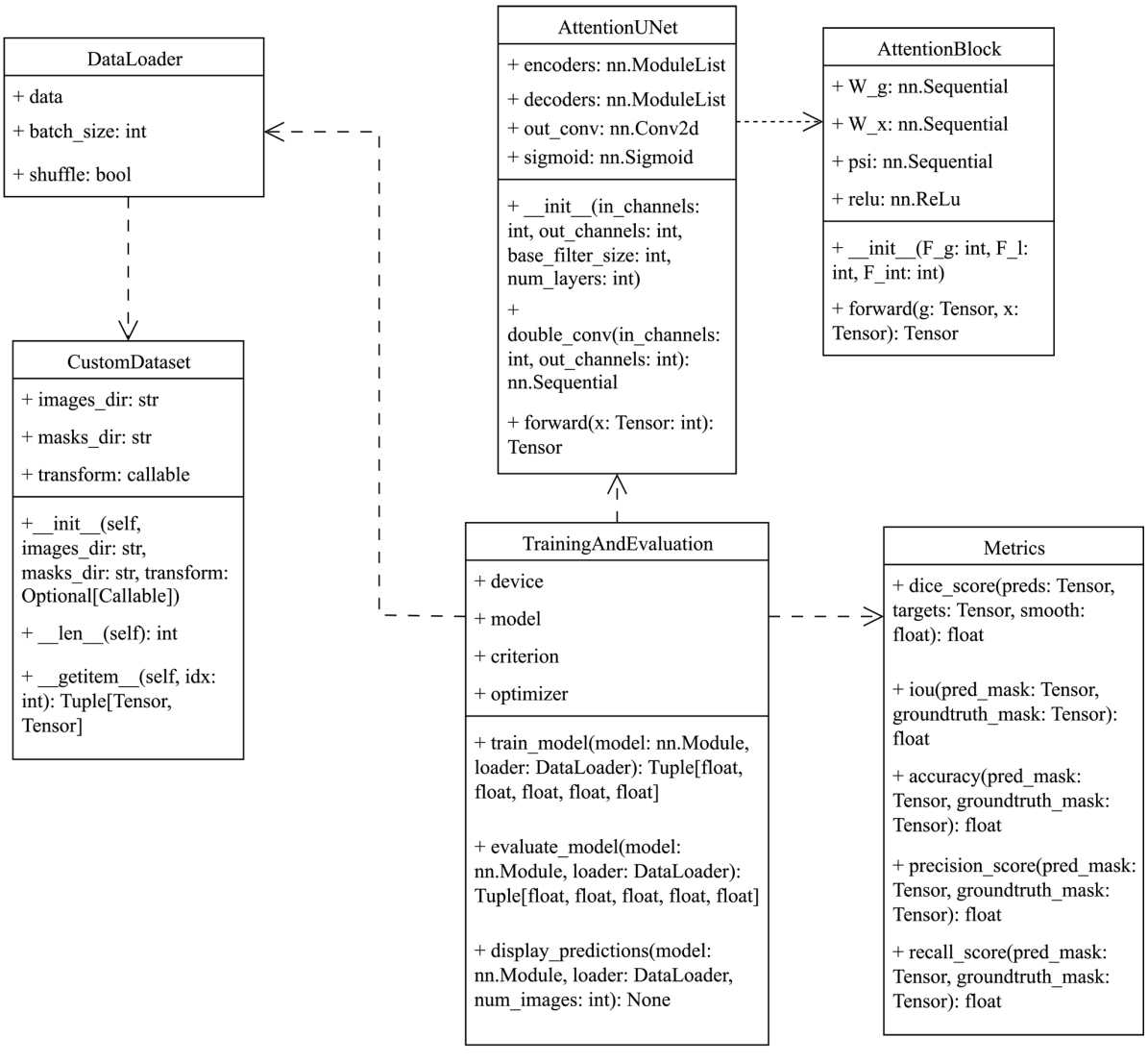

Fig. 9. Segmentation software module class diagram

5. 2. Method for determining the informative parameters of immunohistochemical images and identify breast cancer subtypes automatically

In our study, the U-Net architecture was optimized for segmenting IHC images of breast cancer. Based on this architecture, it was possible to achieve an accuracy of 74%.

In [28], a diagnosing method based on neural networks was devised, the essence of which is the parallel classification and segmentation of biomedical images and the combination of the results into a single formalized report. An integral part of this method is automatic segmentation and formation of a diagnosis based on the calculated informative features that can be obtained from the segmented image.

The general scheme of the method to automatically determine the informative parameters of IHC images and identify breast cancer subtypes is shown in Fig. 10; it consists of the following stages:

1) loading images (original and mask);
2) contour search;
3) visualization (search) of contours;
4) calculation of average intensity;
5) calculation of percentage of positive cells;
6) determining a diagnosis.

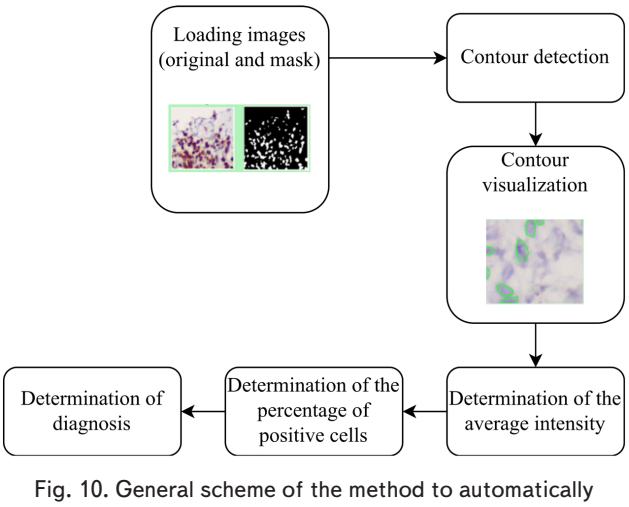

Fig. 10. General scheme of the method to automatically determine the informative parameters and identify breast cancer subtypes

Finding contours is a critical step in transforming a binary segmentation mask into quantitative metrics. The contouring method cv.findContours() from the OpenCV library was used for this purpose. The contour extraction mode cv.RETR_

EXTERNAL and the approximation method cv.CHAIN_APPROX_SIMPLE were selected. Using cv.RETR_EXTERNAL makes it possible to identify only external contours, which is appropriate for counting the number of individual structures, without taking into account internal cavities or nested areas. The resulting contours were used for further calculation of quantitative features, which provided a transition from pixel-based segmentation to interpretable quantitative metrics necessary for accurate identification of breast cancer subtypes.

As described above, one histopathological image corresponds to four immunohistochemical images. Therefore, four images need to be analyzed – one for each biomarker to determine the subtype of breast cancer.

An example of one analyzed image is shown in Fig. 11. The original image is borrowed from [23].

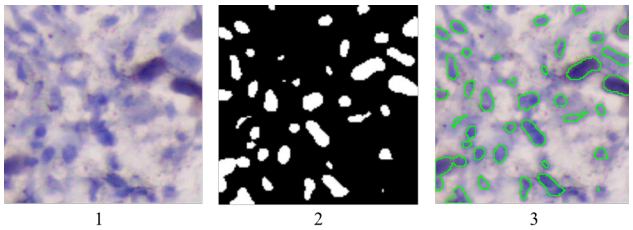

1 2 3

Fig. 11. Example of an analyzed IHC image: 1 — original; 2 — segmented mask; 3 — visualization of contours superimposed on the original image

Based on the obtained image, informative features are calculated, and a diagnosis is defined [25–27] (Fig. 5).

6. Discussion of the results of devising a method for diagnosing breast cancer subtypes automatically

As can be seen from Table 3, increasing the network depth from 4 to 6 layers increased the Dice coefficient from 0.7289 to 0.74. Models with a larger filter size and a smaller depth showed worse results, as this can cause overfitting or lead to an excessive number of parameters without a significant improvement in segmentation quality. The learning rate parameter of 1e-3 showed stable performance for most architectures.

From Fig. 8 it can be seen that the optimized architecture has a greater depth and better ability to analyze features, which generally improves the accuracy of segmentation. Compared to the basic Attention U-Net, which achieved a maximum accuracy of 0.728995, the optimized architecture turned out to be more efficient. This was possible due to the use of a genetic algorithm, which provided a systematic search between the network depth and the size of the basic filter. A depth of 6 layers improved the model's ability to extract more complex features. Reducing the initial filter size to 32 increased localization accuracy and sensitivity to fine details, which is critical for segmenting overlapping or fuzzy kernels. As quantitatively confirmed in Table 5, this configuration not only maximized accuracy but also reduced the variance of the model, indicating a statistically significant advantage over the baseline model.

The advantage of the proposed approach is the comprehensive analysis of architectural changes with experimental confirmation of optimal configurations (Tables 3–5, Fig. 8), which provided an increase in segmentation accuracy compared to the basic Attention U-Net model (DC = 0.7400 versus 0.7289).

In work [17], U-Net for HER2 staining showed 94% in the Accuracy metric and 0.78 in the Dice metric for membrane segmentation, while the proposed method provides Dice = 0.74 for complex IHC images (ER, PR, HER2, Ki67), i.e., with higher variability of tissue types. This indicates a better generalization ability of the model to different biomarkers.

In contrast to [21], in which the GeNSeg-Net model showed Dice in the range of 0.84–0.87, it did not provide subtype diagnosis, working only as a segmenter. The proposed approach, although it has a lower Dice score, nevertheless forms a complete diagnostic chain: segmentation; calculation of quantitative features; subtype classification, which increases the clinical significance of the result.

In [22], 91% accuracy of HER2 classification was achieved, but without the integration of other types of biomarkers and histopathological images. Unlike [22], the approach devised in our study provides a comprehensive analysis of histopathological and IHC images, which ensures completeness of the diagnosis. In addition, the proposed approach does not require the presence of a pathologist to make a diagnosis since it uses clinical guidelines. This provides autonomy in making a diagnosis.

The devised approach demonstrates not only higher stability compared to the basic Attention U-Net but also more comprehensive functionality that covers the full cycle of automatic diagnosis. This makes it practically useful in clinical settings.

Thus, the proposed approach directly solves key problems, namely:

– it provides stable segmentation accuracy when working with different types of biomarkers and histological structures due to adaptive tuning of model parameters;

– it allows for more accurate segmentation of cell nuclei with overlapping or fuzzy boundaries due to an improved architecture that takes into account morphological complexity;

– it improves the identification of fine cellular structures by optimizing the depth and variability of filters, in contrast to classic U-Nets with a fixed scale;

– it provides integrated analysis of histological and IHC images, which increases the accuracy of diagnosis without the mandatory involvement of experts at each stage;

– it is a computationally affordable solution suitable for clinical use in resource-limited environments.

Special features of this study's results are:

– we have devised a comprehensive method for diagnosing breast cancer subtypes automatically, combining the analysis of histopathological and IHC images;

– we have improved the Attention U-Net architecture using a genetic algorithm for the task of segmentation of IHC images, which made it possible to achieve an increase in accuracy;

– we gave devised a method to automatically determine the quantitative features of IHC images based on the results of segmentation for further identification of breast cancer subtypes in accordance with clinical guidelines.

The practical significance of the results is in the applied integration of the designed diagnostic pipeline into the system for diagnosing breast cancer automatically [29]. This reduces the burden on clinicians and increases the objectivity of diagnosis.

However, worth noting are several limitations of the study:

– the efficiency of the designed architecture decreases when the size of the input image increases beyond 512 pixels;

– at high image resolution, problems with a lack of video memory may arise;

– segmentation results depend on the quality of annotations in the training sample.

The disadvantages of the study are the lack of testing on multi-class tasks and limitations on the number of experimental configurations due to available resources.

Further research may include designing an integrated system that combines segmentation, classification, and analysis of informative features with the possibility of adaptation to other types of oncological diseases.

7. Conclusions

1. Attention U-Net has been confirmed to be the most efficient baseline solution (DC = 0.7289). Further optimization of this architecture using a genetic algorithm made it possible to find the optimal configuration (6 layers, baseline filter size 32) and improve the DC indicators to 0.74. The genetic approach provided an increase in accuracy by 1.5% and statistical stability of the model, which is critical for application in clinical practice.

2. A method to automatically determine informative parameters and identify breast cancer subtypes using the optimized architecture has been devised. The method is based on the use of segmented mask contouring with subsequent calculation of quantitative characteristics. A feature of the method and its difference from existing ones is the use of rules and characteristics in accordance with clinical guidelines. The advantage of the method is the possibility of formalized assessment of pathological changes, which makes it possible to improve the consistency of expert assessments.

Conflicts of interest

The authors declare that they have no conflicts of interest in relation to the current study, including financial, personal, authorship, or any other, that could affect the study, as well as the results reported in this paper.

Funding

The study was conducted without financial support.

Data availability

The data cannot be provided for the reasons stated in the data availability statement.

Use of artificial intelligence

The authors used artificial intelligence technologies within acceptable limits to provide their own verified data, which is described in the research methodology section.

Acknowledgments

The authors express their gratitude to the Department of Pathological Anatomy with Section Course and Forensic Medicine at the I. Ya. Horbachevsky Ternopil National Medical University (Ternopil, Ukraine) for providing histological and IHC images of breast cancer.

References

1. Hamet, P., Tremblay, J. (2017). Artificial intelligence in medicine. Metabolism, 69, S36–S40. https://doi.org/10.1016/j.metabol.2017.01.011
2. Briganti, G., Le Moine, O. (2020). Artificial Intelligence in Medicine: Today and Tomorrow. Frontiers in Medicine, 7. https://doi.org/10.3389/fmed.2020.00027
3. Litjens, G., Kooi, T., Bejnordi, B. E., Setio, A. A. A., Ciompi, F., Ghafoorian, M. et al. (2017). A survey on deep learning in medical image analysis. Medical Image Analysis, 42, 60–88. https://doi.org/10.1016/j.media.2017.07.005
4. Srikantamurthy, M. M., Rallabandi, V. P. S., Dudekula, D. B., Natarajan, S., Park, J. (2023). Classification of benign and malignant subtypes of breast cancer histopathology imaging using hybrid CNN-LSTM based transfer learning. BMC Medical Imaging, 23 (1). https://doi.org/10.1186/s12880-023-00964-0
5. Al-Jabbar, M., Alshahrani, M., Senan, E. M., Ahmed, I. A. (2023). Analyzing Histological Images Using Hybrid Techniques for Early Detection of Multi-Class Breast Cancer Based on Fusion Features of CNN and Handcrafted. Diagnostics, 13 (10), 1753. https://doi.org/10.3390/diagnostics13101753
6. Miranda Ruiz, F., Lahrmann, B., Bartels, L., Krauthoff, A., Keil, A., Härtel, S. et al. (2023). CNN stability training improves robustness to scanner and IHC-based image variability for epithelium segmentation in cervical histology. Frontiers in Medicine, 10. https://doi.org/10.3389/fmed.2023.1173616
7. Zaha, D. C. (2014). Significance of immunohistochemistry in breast cancer. World Journal of Clinical Oncology, 5 (3), 382. https://doi.org/10.5306/wjco.v5.i3.382
8. Aswathy M. A., Mohan, J. (2020). Analysis of Machine Learning Algorithms for Breast Cancer Detection. Handbook of Research on Applications and Implementations of Machine Learning Techniques, 1–20. https://doi.org/10.4018/978-1-5225-9902-9.ch001
9. Nabok, A. I. (2023). Prevalence and incidence of breast cancer in Ukraine. Wiadomości Lekarskie, 76 (10), 2219–2223. Available at: https://www.researchgate.net/profile/Serhii-Tertyshnyi/publication/375025887_WL_Layout_10_2023/links/653bdaf73cc79d48c5b14c25/WL-Layout-10-2023.pdf#page=93
10. Siegel, R. L., Kratzer, T. B., Giaquinto, A. N., Sung, H., Jemal, A. (2025). Cancer statistics, 2025. CA: A Cancer Journal for Clinicians, 75 (1), 10–45. https://doi.org/10.3322/caac.21871
11. Ronneberger, O., Fischer, P., Brox, T. (2015). U-Net: Convolutional Networks for Biomedical Image Segmentation. Medical Image Computing and Computer-Assisted Intervention – MICCAI 2015, 234–241. https://doi.org/10.1007/978-3-319-24574-4_28

12. Polley, M.-Y. C., Leung, S. C. Y., McShane, L. M., Gao, D., Hugh, J. C., Mastropasqua, M. G. et al. (2013). An International Ki67 Reproducibility Study. JNCI: Journal of the National Cancer Institute, 105 (24), 1897–1906. https://doi.org/10.1093/jnci/djt306
13. Kumar, N., Gupta, R., Gupta, S. (2020). Whole Slide Imaging (WSI) in Pathology: Current Perspectives and Future Directions. Journal of Digital Imaging, 33 (4), 1034–1040. https://doi.org/10.1007/s10278-020-00351-z
14. Siddique, N., Paheding, S., Elkin, C. P., Devabhaktuni, V. (2021). U-Net and Its Variants for Medical Image Segmentation: A Review of Theory and Applications. IEEE Access, 9, 82031–82057. https://doi.org/10.1109/access.2021.3086020
15. Mehta, R., Arbel, T. (2019). 3D U-Net for Brain Tumour Segmentation. Brainlesion: Glioma, Multiple Sclerosis, Stroke and Traumatic Brain Injuries, 254–266. https://doi.org/10.1007/978-3-030-11726-9_23
16. Chen, W., Liu, B., Peng, S., Sun, J., Qiao, X. (2019). S3D-UNet: Separable 3D U-Net for Brain Tumor Segmentation. Brainlesion: Glioma, Multiple Sclerosis, Stroke and Traumatic Brain Injuries, 358–368. https://doi.org/10.1007/978-3-030-11726-9_32
17. Benny, S., Varma, S. L. (2021). Semantic Segmentation in Immunohistochemistry Breast Cancer Image using Deep Learning. 2021 International Conference on Advances in Computing, Communication, and Control (ICAC3), 1–3. https://doi.org/10.1109/icac353642.2021.9697264
18. Benny, S., Varma, S. L. (2023). Attention-enhanced residual U-Net for nucleus segmentation in immunohistochemistry images. International Journal of Applied Engineering & Technology, 5 (4), 1266–1283. Available at: https://romanpub.com/resources/ijaet20v5-4-2023-138.pdf
19. Mahanta, L. B., Hussain, E., Das, N., Kakoti, L., Chowdhury, M. (2021). IHC-Net: A fully convolutional neural network for automated nuclear segmentation and ensemble classification for Allred scoring in breast pathology. Applied Soft Computing, 103, 107136. https://doi.org/10.1016/j.asoc.2021.107136
20. Kromp, F., Fischer, L., Bozsaky, E., Ambros, I. M., Dorr, W., Beiske, K. et al. (2021). Evaluation of Deep Learning Architectures for Complex Immunofluorescence Nuclear Image Segmentation. IEEE Transactions on Medical Imaging, 40 (7), 1934–1949. https://doi.org/10.1109/tmi.2021.3069558
21. Xu, S., Li, G., Song, H., Wang, J., Wang, Y., Li, Q. (2024). GeNSeg-Net: A General Segmentation Framework for Any Nucleus in Immunohistochemistry Images. Proceedings of the 32nd ACM International Conference on Multimedia, 4475–4484. https://doi.org/10.1145/3664647.3681441
22. Aboudessouki, A., Ali, Kh. M., Elsharkawy, M., Alksas, A., Mahmoud, A., Khalifa, F. et al. (2023). Automated Diagnosis of Breast Cancer Using Deep Learning-Based Whole Slide Image Analysis of Molecular Biomarkers. 2023 IEEE International Conference on Image Processing (ICIP). https://doi.org/10.1109/icip49359.2023.10222479
23. Tkachova, O. V., Melnyk, H. M., Pitsun, O. Y., Datsko, T. V., Klishch, I. M., Derysh, B. B. (2023). A. s. No. 118979. Baza danykh tsyfrovykh imunohistokhimichnykh zobrazhen raku molochnoi zalozy "IHCDBI". declareted: 10.05.2023; published: 31.07.2023, Bul. No. 76.
24. Huynh, N. (2023). Understanding evaluation metrics in Medical Image Segmentation. Available at: https://medium.com/mastering-data-science/understanding-evaluation-metrics-in-medical-image-segmentation-d289a373a3f
25. WBRT pislia BCS. Rak molochnoi zalozy na rannikh stadiyakh: Klinichna nastanova, zasnovana na dokazakh (2024). Ministerstvo okhorony zdorovia Ukrainy, 27–28. Available at: https://www.dec.gov.ua/wp-content/uploads/2025/02/kn_2025_rannij-rmz.pdf
26. Berezsky, O., Pitsun, O., Melnyk, G., Datsko, T., Izonin, I., Derysh, B. (2023). An Approach toward Automatic Specifics Diagnosis of Breast Cancer Based on an Immunohistochemical Image. Journal of Imaging, 9 (1), 12. https://doi.org/10.3390/jimaging9010012
27. Cardoso, F., Kyriakides, S., Ohno, S., Penault-Llorca, F., Poortmans, P., Rubio, I. T. et al. (2019). Early breast cancer: ESMO Clinical Practice Guidelines for diagnosis, treatment and follow-up. Annals of Oncology, 30 (8), 1194–1220. https://doi.org/10.1093/annonc/mdz173
28. Liashchynskyi, P. B., Berezsky, O. M. (2024). Computer diagnostic systems: methods and tools. Ukrainian Journal of Information Technology, 6 (2), 57–63. https://doi.org/10.23939/ujit2024.02.057
29. Berezsky, O. M., Liashchynskyi, P. B. (2024). Development of the architecture of a computer aided diagnosis system in medicine. Applied Aspects of Information Technology, 7 (4), 359–369. https://doi.org/10.15276/aait.07.2024.25